Engineering in Agriculture, Environment and Food xxx (xxxx) xxx–xxx

Contents lists available at ScienceDirect

Engineering in Agriculture, Environment and Food

journal homepage: www.elsevier.com/locate/eaef

Observation and analysis of internal structure of cucumber fruit during storage using X-ray computed tomography

Fumihiko Tanaka[a,*], Kohei Nashiro[b], Wako Obatake[b], Fumina Tanaka[a], Toshitaka Uchino[a]

[a] Laboratory of Postharvest Science, Faculty of Agriculture, Kyushu University, 6-10-1, Hakozaki, Higashi-ku, Fukuoka 812-8581, Japan
[b] Graduate School of Bioresource and Bioenvironmental Sciences, Kyushu University, 6-10-1, Hakozaki, Higashi-ku, Fukuoka 812-8581, Japan

ARTICLE INFO

Keywords:
Cucumber
X-ray computed tomography
Image processing
Physical properties

ABSTRACT

In this study, X-ray computed tomography (CT) was used as a non-destructive technique to characterize and quantify the internal structure of cucumber fruit during storage. The physical properties of cucumber fruit were also measured destructively and related to X-ray absorptivity, and also changes in three-dimensional heterogeneous internal structure were visualized during storage at 15 °C and 25 °C and 90% RH for 7 days. As a result, the average gray scale (GS) value calculated from X-ray CT scanned tissue images indicated good correlations with the density, porosity, and elastic modulus of cucumber fruit. The peak height of the GS value related to the density and porosity. Standard deviation of the GS value was also related to the moisture content of the fruit. These results indicated that X-ray CT can be used to estimate physical properties related fruit quality. It was also revealed that the radiodensity of cucumber fruit changed in the mesocarp tissue but not change in the placenta tissue. GS level in the mesocarp tissue changed from white to dark from the fruit pedicel towards the apex at 25 °C. This result is useful to understand the expansion of low density part in fruit during storage.

1. Introduction

The evaluation of internal quality of fresh produce is extremely important for the agricultural industry and consumers, and numerous non-destructive imaging methods have been developed in recent years. X-ray computed tomography (CT) is a useful technique for non-distractive mapping of radiodensity distribution, and it provides high-quality images of the internal structure of agricultural produce because the differences in X-ray attenuation of different materials creates contrast to differentiate low- and high-density materials (Karathanasis and Hajek, 1996). X-ray imaging techniques have been widely used in the agricultural and food industry for foreign material detection and quality control. Morita et al. (2003a, 2003b) proposed a foreign material detection method for food by spectral analysis of reflected soft X-rays, and Arendse et al. (2016, in press) measured the geometrical characters (volume and size) of pomegranate fruit. In addition, Kelkar et al. (2015) proposed a method to determine the density of foods using X-ray linear attenuation. Moreover, Jha et al. (2010) reported the potential of X-ray CT to characterize the internal and external properties of mango. Donis-González et al. (2014a) investigated the internal decay of chestnuts, internal defects in pickling cucumbers, translucency disorder in pineapple, pit presence in tart cherries and plum curculio infestation of tart cherries. They suggested that there is a potential for non-destructive inline sorting of the internal quality of several agricultural products. Donis-González et al. (2014b) developed the classification method based on CT images for fresh chestnuts. Donis-González et al. (2015) also investigated the presence of undesirable fibrous tissue in carrots through CT images. Using high resolution CT, the pore space within apple (Mendoza et al., 2007), core breakdown in pears (Lammertyn et al., 2003a, 2003b), microstructure in kiwifruit (Cantre et al., 2014) and bread (Demirkesen et al., 2014) were investigated. Verboven et al. (2008) visualized three-dimensional gas exchange pathway in pome fruit using synchrotron radiation X-ray tomography. Kuroki et al. (2004) investigated that gas-filled intercellular spaces in cucumber fruit were developed after harvest; however, there is no investigation of internal structure change in whole fruit during storage. And previous studies have so far not focused on using X-ray imaging to directly determine the physical properties of fruit during storage.

The objectives of this study were to relate the physical properties of cucumber fruit to X-ray CT attenuation characteristics and to visualize three-dimensional heterogeneous structural changes in the fruit during storage.

* Corresponding author.
E-mail address: fumit@bpes.kyushu-u.ac.jp (F. Tanaka).

https://doi.org/10.1016/j.eaef.2017.12.004
Received 17 July 2016; Received in revised form 12 August 2017; Accepted 18 December 2017

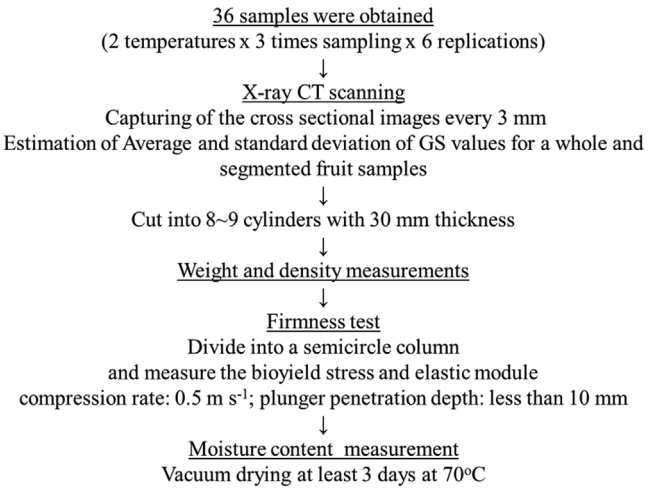

Fig. 1. Flowchart of experiments.

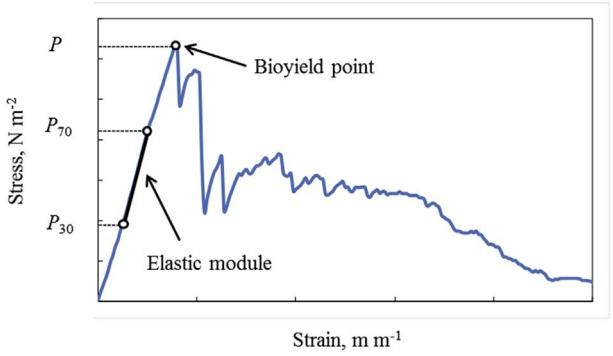

Fig. 2. Definition of firmness of cucumber fruit.

2. Materials and methods

2.1. Material and storage conditions

Fresh cucumber fruit (*Cucums sativus* L.) picked at the proper stage of maturity were obtained from a local market and stored in a low-temperature and humidity chamber (TPAV-120-20, ISUZU, Niigata, Japan) at 15 °C or 25 °C with 90% relative humidity (RH) for 7 days. Storage experiment at 25 °C was employed as an accelerated aging test. All samples were assessed for density, porosity, moisture content, flesh firmness, and X-ray attenuation at day 1 (initial day), day 4, and day 7 (some data were also obtained at day 3 and day 5). The samples for measuring physical properties were cut into 30 mm lengths in order to describe the differences along the fruit from pedicel to apex and were divided into 8–9 segments. Fig. 1 shows a flowchart of the X-ray CT scanning and physical properties experiments. Totally, 36 cucumbers were used to relate the X-ray CT and physical properties. The procedures and methods were detailed in the following sections.

2.2. Measurement of physical properties

2.2.1. Density and porosity

Density was measured by the water replacement method and a pycnometer method, respectively. To estimate the density of segmented cucumber, the sample volume V_s (m^3) was measured by the water replacement method at 25 °C. Density ρ_s (kg m^{-3}) was calculated using the following equation (1):

$$\rho_s = m_s/V_s \quad (1)$$

where m_s is the sample mass (kg).

True density ρ_{tr} (kg m^{-3}) was measured using a pycnometer method with toluene as the displacement medium at 25 °C. Then, porosity ε was calculated using the following equation (2):

$$\varepsilon = 1 - \rho_s/\rho_{tr} \quad (2)$$

2.2.2. Flesh firmness

Bioyield stress and elastic modulus of samples were measured using a creep meter (RE-3305, YAMADEN, Tokyo, Japan) equipped with a cylindrical plunger (diameter: 3 mm) was used for the puncture test. The samples were cut into 30 mm thickness along its length and the shape of a semicircle column was obtained by cutting a column in half in the direction of height to measure flesh firmness. The sample was placed on the stage of the creep meter with the cut surface on the base plate and the plunger penetrated up to 10 mm into the sample at a speed of 0.5 mm s^{-1}. In accordance with the texture analysis method proposed by Mallikarjunan (2011), the bioyield stress P_b (N m^{-2}) and elastic modulus E (N m^{-2}) of sample were estimated from the stress-strain curve as described in Fig. 2. E was calculated from the slope between the points given the stress P_{70} and P_{30} in the stress-strain curve (see Fig. 2).

2.2.3. Moisture content

In order to measure the moisture content (wet basis, w.b.) of cucumber, each cut samples with 30 mm thickens was placed in an aluminum cup and dried for at least 3 days at 70 °C in a vacuum oven (ADP 300, Yamato Scientific Co., Tokyo, Japan) with a vacuum pump (Minivac PD-138, Yamato Scientific Co., Tokyo, Japan: Attainable vacuum 0.062 Pa, effective exhaust speed 162 L min^{-1}).

2.3. X-ray computed tomography measurement

X-ray CT images were generated using an X-ray CT scanner (Latheta LCT-100, Hitachi Aloka Medical, Tokyo, Japan) with X-ray source operated at 50 kV and 1 mA. Entire cucumber was placed in a holder with a 120 mm inner diameter and scanned using a slice thickness of 3 mm at the scanning and computation time of 18 s/slice. A series of sliced images was captured from the fruit apex towards the pedicel. About 70 images were obtained from each sample and the pixel resolution was 250 μm (480 × 480 pixels/image). The Hounsfield Unit (HU) scale was employed to express X-ray attenuation through the sample. In the HU scale, the radiodensity of distilled water at standard pressure and temperature is defined as zero HU, while the radiodensity of air at standard pressure and temperature is defined as −1000 HU. The corresponding HU value can be defined as:

$$HU = 1000 \times (\mu - \mu_{water})/(\mu_{water} - \mu_{air}) \cong 1000 \times (\mu - \mu_{water})/\mu_{water} \quad (3)$$

where μ (cm^{-1}), μ_{water} (cm^{-1}) and μ_{water} (cm^{-1}) are the linear attenuation coefficients of sample, air and water, respectively (Huda, 2010). After adjusting the HU scales range, each slice image was stored as 8-bit bitmap (480 × 480 pixels). The scanning was replicated three times for each condition.

2.4. Image processing

Image J software (NIH) was used for digital image processing. HU can be simply converted to 8-bit digital data; however, it is necessary to identify an adequate range of HU values in order to visualize the slice image without noise. To obtain a clear X-ray CT image, an adequate HU range was identified. When the binary image was obtained without limiting the HU range, noise could not be removed. When a lower limit was set at −850 HU, a void area appeared inside the cucumber fruit on day 1. As for a higher HU limitation, 300 HU was employed because there was no noise data surrounding the fruit over than this threshold value. Therefore, a range from −900 to 300 HU was employed to

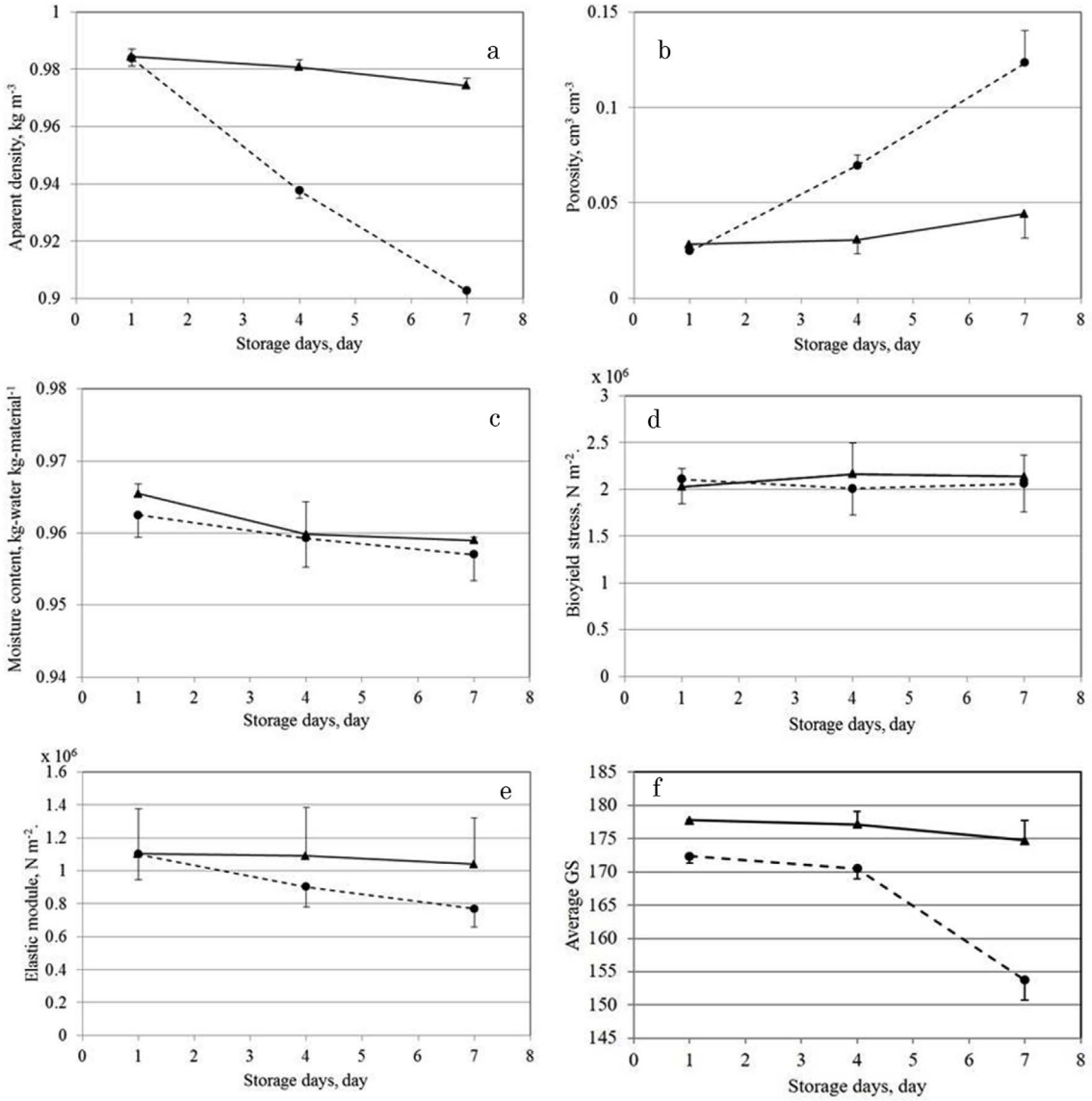

Fig. 3. Changes in the average physical properties and gray scale value during storage at 15 °C (solid line) and 25 °C (dotted line) with 90% RH for 7 days.

Fig. 4. Extracted binary CT images at different thresholding levels.

extract cucumber fruit features, and the GS value was estimated. The HU scale was converted linearly to an 8-bit gray scale (*GS*) digital image.

$$GS = 255 \times (HU + 900)/1200 \quad (4)$$

Then, the radiodensity of distilled water and air at standard pressure and temperature were 191 and 0, respectively. The average GS value was determined for each 30 mm segmented sample from fruit apex towards the pedicel using ten continuous images except for the final region because of a lack of sufficient length. The histogram of GS value was also calculated for whole fruit during storage in different conditions. The relationships between the statistical analysis data for image and the physical properties were investigated for different storage conditions.

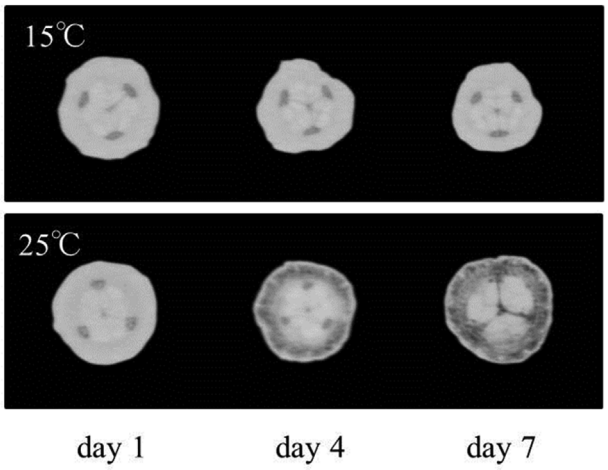

Fig. 5. Changes of cucumber fruit structure based on X-ray CT image at different storage temperatures.

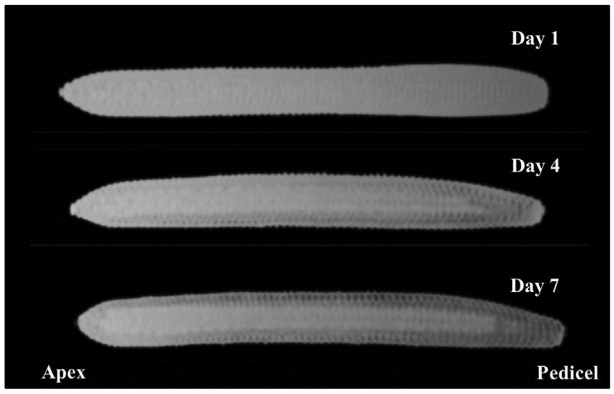

Fig. 6. Three-dimensional internal structure change of cucumber fruit during storage at 25 °C with 90% RH for 7 days.

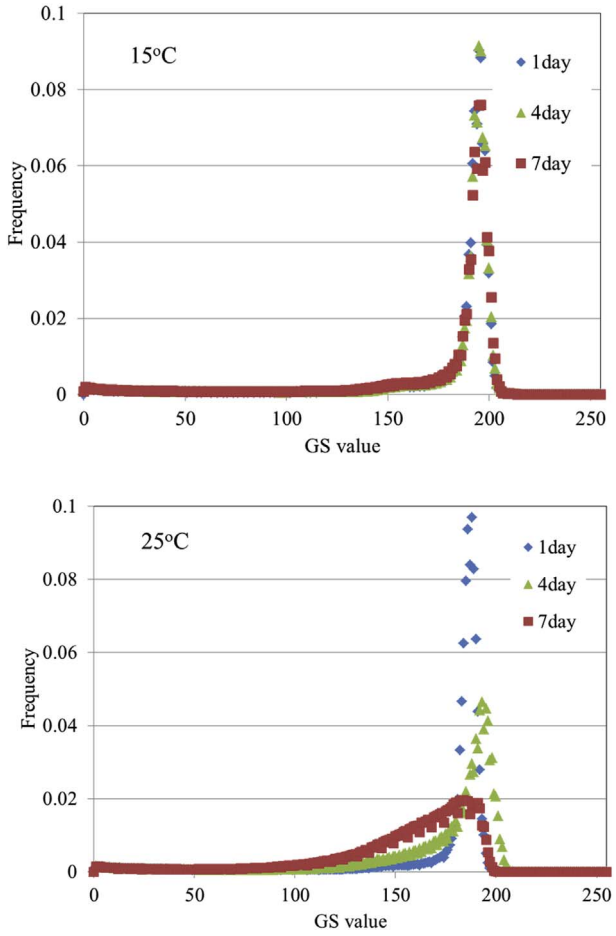

Fig. 7. Changes in GS value histogram for a whole cucumber fruit during storage at different temperatures.

3. Result and discussion

3.1. Physical properties

Changes in density, porosity, moisture content, and flesh firmness (bioyield stress and elastic module) were measured during 7 days of storage at 15 °C and 25 °C and 90% RH. The samples were cut into 30 mm length segments. The physical properties were measured for each segmented sample and were averaged to obtain the mean values. Changes in the mean density, porosity, moisture content, bioyield stress, elastic module, and GS values for each whole fruit are shown in Fig. 3a–e. The mean density decreased continuously, and the decrease was more significant at 25 °C (Fig. 3a). On the other hand, the mean porosity increased continuously and the increase was more significant at 25 °C (Fig. 3b). The initial porosity was around 3% and the result was similar to that obtained by Kuroki et al. (2004). The density and porosity were strongly correlated together. It means the true density did not change and it was around 1010 kg m^{-3}. The mean moisture content decreased continuously; however, a significant difference was not recognized at either temperature (Fig. 3c). Shikiyama and Nakamura (1976), Shikiyama et al. (1978), and Kuroki et al. (2004) suggested that the volume of whole fruit decreased for about 3 days after harvest, but then increased in synchrony with the change in appearance during storage at 20 °C. Therefore, a greater decrease in density and increase in porosity might be observed at 25 °C, even though there was not much different in moisture content. As for storage at 15 °C, there were few changes in density, porosity and moisture content. Fig. 3d and e shows changes in bioyield stress and elastic modules, respectively. The bioyield stress did not change at either temperature, whereas the elastic module decreased at 25 °C during storage for 7 days. As for bioyield stress, it may indicate the hardness of the exocarp because the skin was broken when the bioyield point was observed. The elastic module also indicates the hardness of the skin or exocarp of cucumber because the slope data in Fig. 2 are fundamentally come from skin or exocarp of cucumber. The elastic module decreased significantly at 25 °C.

3.2. X-ray computed tomography measurements

Fig. 4 shows binary CT images extracted by assuming −1000, −900 and −850 HU for the lower limits of the threshold for the original images captured using an X-ray CT scanner. As shown in section 2.4, when a lower limit was set at −1000 HU, image noise in surroundings of the cucumber fruit appeared. If a lower limit was set at −850 HU, a void area appeared inside the fruit on day 1. At a lower threshold of −900 HU, the noise and void area were removed perfectly. A higher threshold of 300 HU was employed because there was no noise data surrounding the fruit over then this threshold. In this study, a range from −900 to 300 HU was employed to extract cucumber fruit features. And also Fig. 5 illustrates the changes in features based on GS images at 9 cm from the fruit apex during 7 days of storage at 15 and 25 °C. A remarkable difference in GS images was observed only at 25 °C storage. The GS value decreased in the endocarp and mesocarp tissue, but a significant change in GS was not found in the placenta tissue. Fig. 6 shows a three-dimensional structure visualized from a stacked series of 2D CT images captured on day 1, day 4, and day 7 for a whole fruit stored at 25 °C. These were different fruits taken out of the storage for each day. It was observed that the GS picture in mesocarp tissue

Table 1
Correlation coefficient between the average GS value and physical properties.

Density	Porosity	Moisture content	Bioyield	Elastic module
0.885	−0.869	0.124	0.0794	0.574

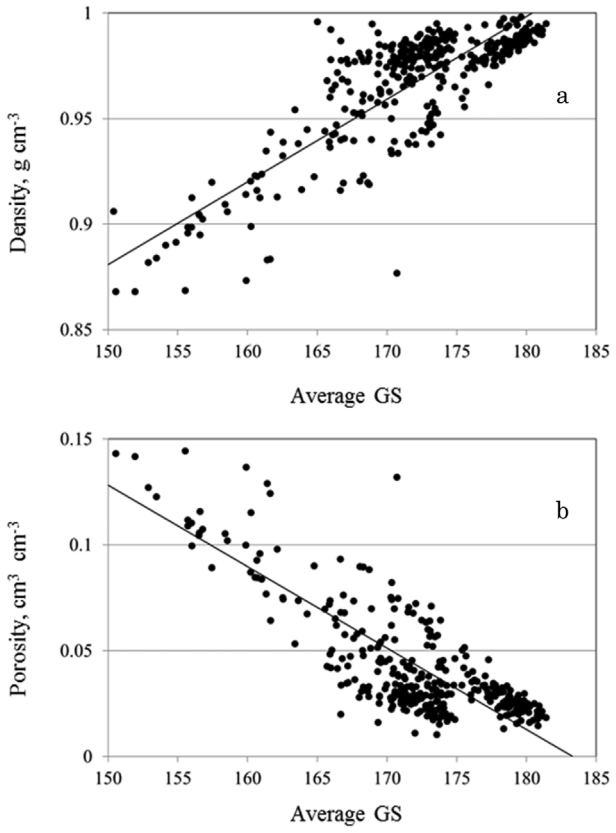

Fig. 8. The density and Porosity of segmented samples dependencies on average GS value.

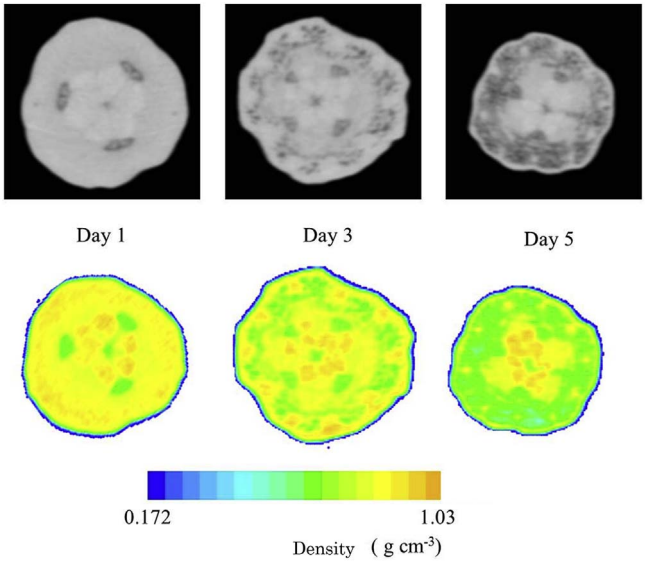

Fig. 9. Predicted density distribution at 25 °C storage by equation (5).

changed from white to dark from the fruit pedicel towards the apex during storage; however, GS did not change in the placenta tissue. It was concluded that the radiodensity of cucumber fruit changed in the mesocarp tissue, but it did not change in the placenta tissue during 7 days of storage at 25 °C. Fig. 7 shows a histogram of GS values for whole fruit stored at two different temperatures for 7 days. The shape of the histogram did not change at 15 °C, whereas it spread wider towards to lower GS values and the height of the peak decreased with increasing storage time. The peak of GS was located around 190 because the radiodensity of distilled water at standard pressure and temperature was 191. The shape of the histogram may have strong relation to the physical properties of the fruit, because the GS value of each pixel was estimated in accordance with the component ratio of water, air, and other materials. Changes in the average GS value for a whole fruit are shown in Fig. 3f. The average GS value decreased continuously and the decrease was more significant at 25 °C.

3.3. Relationship between physical properties and X-ray computed tomography feature values

The absorption of X-rays follows Lambert–Beer's law (Jackson and Hawkes, 1981). Because the attenuation coefficient in the equation is dependent on the density of the material (Falcone et al., 2005; Kelkar et al., 2015), it is expected that the GS picture may provide useful information on the physical properties of cucumber fruit without destructive sampling. In this section, we investigated the relationship between physical properties and X-ray CT feature values. Table 1 shows the correlation coefficients between the physical properties and the average GS values for all conditions. The physical properties were measured for each 30 mm thick section, and the average GS values were also determined for each 30 mm segmented region from the fruit apex towards the pedicel using ten continuous images. Every pixel that formed the CT image was assessed for its individual GS value in the density of the corresponding region. The GS values obtained from the cucumber samples correlated quite highly with the density (r = 0.885) and porosity (r = −0.869), as shown in Figure 8(a), (b) and Table 1. The following linear relationships were obtained.

$$\rho_s = 3.92 \times 10^{-3} GS + 2.93 \times 10^{-1} \quad (5)$$

$$\varepsilon = 3.85\times10^{-3}\, GS + 7.05\times10^{-1} \quad (6)$$

As an example of the physical property estimation based on CT data, the predicted density distributions are illustrated in Fig. 9. There is some possibility of estimating the actual density of cucumber fruit. At the outer circumference of fruit, the estimated density showed extremely smaller value because the outer pixel involved air and skin.

The average GS value did not correlate with moisture content contrary to expectation (r = 0.124). For flesh firmness, bioyield stress did not correlate with the average GS value (r = 0.0794) because the mechanical properties depended on the hardness of the skin or exocarp. In contrast, elastic module had weak correlation with the average GS value (r = 0.574). However, it is mainly dependent on the firmness of the skin or exocarp of cucumber because the slope data in Fig. 2 are fundamentally come from skin or exocarp of cucumber.

Other potential features of the CT were investigated, and the following relations were obtained.

$$\rho_s = 6.575 \times 10^{-7} e^{12.0610 GS_p} \quad (r = 0.920)$$

$$\varepsilon = 4.534 \times 10^{-2} \ln GS_p - 0.06698 \quad (r = -0.925)$$

$$M = -7.195 \times 10^{-4} GS_{sd} + 0.9896 \quad (r = 0.570)$$

where the subscript p and sd indicate the peak and standard deviation of GS distribution. As a result, it appeared that the density and porosity of cucumber fruit could be estimated using the peak height value of GS as well as the average GS value. Furthermore, the possibility of moisture content prediction based on the standard deviation of the GS value distribution was indicated. The standard deviation of the GS value has weak correlation with the moisture content of the fruit. Further investigation is needed to predict the moisture content

distribution in cucumber fruit accurately.

4. Conclusion

In this study, changes in the physical properties of cucumber fruit were measured during storage at 15 °C and 25 °C with 90% RH for 7 days and related to X-ray CT features. The results are summarized as follows:

(1) Density, elastic module, and average GS value decreased whereas porosity increased during storage only at 25 °C.
(2) The radiodensity of cucumber fruit changed in the endocarp and mesocarp tissues, but it did not change in the placenta tissue during 7 days of storage at 25 °C. In three-dimensional GS mapping, the GS level in the endocarp and mesocarp tissues changed from white to dark from the fruit pedicel towards the apex at 25 °C.
(3) GS value and the peak height of the GS histogram correlated quite highly with the apparent density and porosity of the fruit.
(4) It was observed that GS value has weak correlation with the elastic module of the fruit.
(5) The standard deviation of the GS value has weak correlation with the moisture content of the fruit.

This work demonstrates that X-ray CT can be applied to estimate the physical properties of cucumber fruit without destructive sampling.

Acknowledgments

This work was supported by JSPS KAKENHI Number JP26292135 and JP15K14836.

References

Arendse, E., Fawole, O.A., Magwaza, L.S., Opara, U.L., 2016. Non-destructive characterization and volume estimation of pomegranate fruit external and internal morphological fractions using X-ray computed tomography. J. Food Eng. 186, 42–49.
Cantre, D., East, A., Verboven, P., Araya, X.T., Herremans, E., Nicolaï, B.M., Pranamornkith, T., Loh, M., Mowat, A., Heyes, J., 2014. Microstructural characterisation of commercial kiwifruit cultivars using X-ray micro computed tomography. Postharvest Biol. Technol. 92, 79–86.
Demirkesen, I., Kelkar, S., Campanella, O.H., Sumnu, G., Sahin, S., Okos, M., 2014. Characterization of structure of gluten-free breads by using X-ray microtomography. Food Hydrocolloids 36, 37–44.
Donis-González, I.R., Guyer, D.E., Pease, A., Barthel, F., 2014a. Internal characterisation of fresh agricultural products using traditional and ultrafast electron beam X-ray computed tomography imaging. Biosyst. Eng. 117, 104–113.
Donis-González, I.R., Guyer, D.E., Fulbright, D.W., Pease, A., 2014b. Postharvest non-invasive assessment of fresh chestnut (*Castanea* spp.) internal decay using computer tomography images. Postharvest Biol. Technol. 94, 14–25.
Donis-González, I.R., Guyer, D.E., Chen, R., Pease, A., 2015. Evaluation of undesirable fibrous tissue in processing carrots using Computed Tomography (CT) and structural fiber biochemistry. J. Food Eng. 153, 108–116.
Falcone, P.M., Baiano, A., Zanini, F., Mancini, L., Tromba, G., Dreossi, D., Montanari, F., Scuor, N., Del Nobile, M.A., 2005. Three-dimensional quantitative analysis of bread crumb by X-ray microtomography. J. Food Sci. 70 (4), E265–E272.
Huda, W., 2010. Review of Radiologic Physics. Lippincott Williams & Wilkins, PA, USA.
Jackson, D.F., Hawkes, D.J., 1981. X-ray attenuation coefficients of elements and mixtures. Phys. Rep. 70 (3), 169–233.
Jha, S.N., Narsaiah, K., Sharma, A.D., Singh, M., Bansal, S., Kumar, R., 2010. Quality parameters of mango and potential of non-destructive techniques for their measurement – a review. J. Food Sci. Technol. 47, 1–14.
Karathanasis, A.D., Hajek, B.F., 1996. Elemental analysis by X-ray fluorescence spectroscopy. In: Sparks, D.L. (Ed.), Methods of Soil Analysis. Soil Science Society of America, Madison, WI, pp. 161–223.
Kelkar, S., Boushey, C., Okos, M., 2015. A method to determine the density of foods using X-ray imaging. J. Food Eng. 159, 36–41.
Kuroki, S., Oshita, S., Sotome, I., Kawagoe, Y., Seo, Y., 2004. Visualization of 3-D network of gas-filled intercellular spaces in cucumber fruit after harvest. Postharvest Biol. Technol. 33, 255–262.
Lammertyn, J., Dresselaers, T., Van Hecke, P., Jancsók, P., Wevers, M., De Baerdemaeker, J., Nicolaï, B.M., 2003a. MRI and X-ray CT study of spatial distribution of core breakdown in 'Conference' pears. Magn. Reson. Imag. 21, 805–815.
Lammertyn, J., Dresselaers, T., Van Hecke, P., Jancsók, P., Wevers, M., De Baerdemaeker, J., Nicolaï, B.M., 2003b. Analysis of the time course of core breakdown in 'Conference' pears by means of MRI and X-ray CT. Postharvest Biol. Technol. 29, 19–28.
Mallikarjunan, P.K., 2011. Physical measurements. In: Sun, D.-W. (Ed.), Handbook of Frozen Food Processing and Packaging. CRC Press, Boca Raton, FL, pp. 549–562.
Mendoza, F., Verboven, P., Mebatsion, H.K., Kerckhofs, G., Wevers, M., Nicolaï, B., 2007. Three-dimensional pore space quantification of apple tissue using X-ray computed microtomography. Planta 226, 559–570.
Morita, K., Ogawa, Y., Thai, C.N., Tanaka, F., 2003a. Soft X-ray image analysis to detect foreign materials in food. Food Sci. Technol. Res. 9 (2), 137–141.
Morita, K., Ogawa, Y., Thai, C.N., Tanaka, F., Ishiguro, E., 2003b. Spectral analysis of reflected soft X-ray for detecting foreign materials in food. Food Sci. Technol. Res. 9 (2), 231–236.
Shikiyama, R., Nakamura, S., 1976. Change in volume and specific gravity of cucumber fruits after harvest in relation to the recovery from a flaccid appearance. Sci. Hortic. 5, 303–310.
Shikiyama, R., Nakamura, Y., Nakamura, S., 1978. Effect of parthenocarpy, peeling and fruit age on the changes in volume and specific gravity of cucumber fruits during storage at 20 °C.
Verboven, P., Kerckhofs, G., Mebatsion, H.K., Ho, Q.T., Temst, K., Wevers, M., Cloetens, P., Nicolai, B.M., 2008. Three-dimensional gas exchange pathways in pome fruit characterized by synchrotron x-ray computed tomography. Plant Physiol. 147, 518–527.